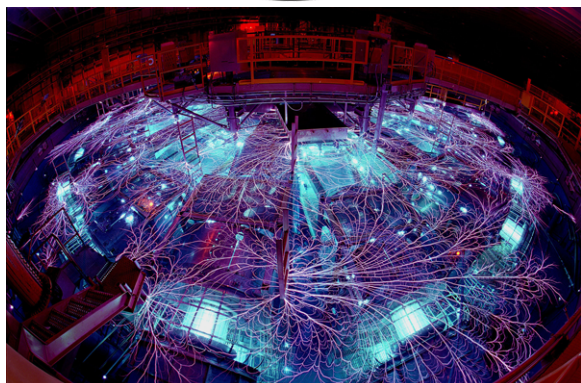


Exceptional service in the national interest



Impact of magnetic fields on tail-ion kinetics in ICF plasma

Paul F. Schmit
Los Alamos National Laboratory
June ##, 2013



Sandia National Laboratories is a multi-program laboratory managed and operated by Sandia Corporation, a wholly owned subsidiary of Lockheed Martin Corporation, for the U.S. Department of Energy's National Nuclear Security Administration under contract DE-AC04-94AL85000.

Acknowledgments

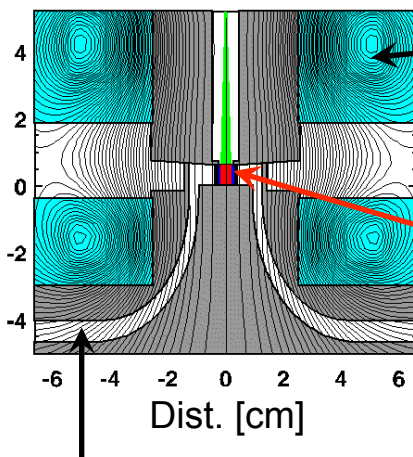
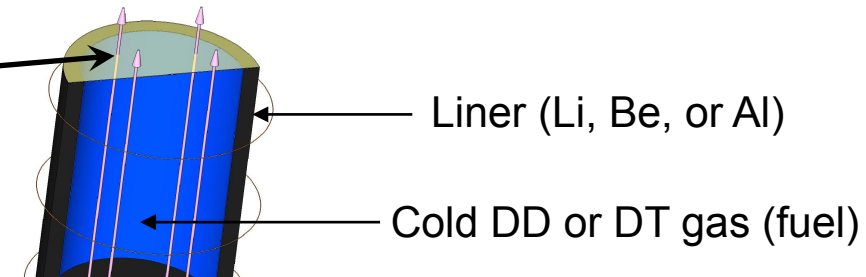
Special thanks to Kim Molvig (LANL), Evan Dodd (LANL), and Charles Nakhleh (SNL) for their input and guidance during the course of this project.

Outline

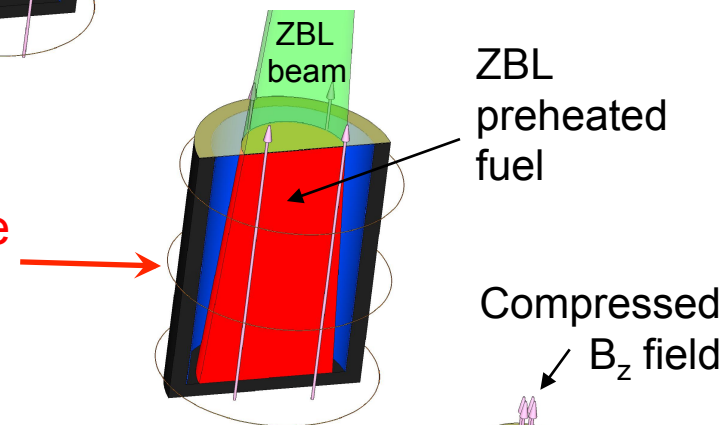
- Magnetized and cylindrical ICF systems
- Overview of Knudsen loss mechanism
- Heuristic model illustrating impact of applied magnetic field
- Full kinetic equations and model assumptions
- New SDE tail-ion transport particle code
- Qualitative effects of B-field on tail-ion transport
- Exploring the dimensionless parameter landscape
- Ion distribution function anisotropy/inhomogeneity
- Conclusions and future work

We are working toward the evaluation of a new Magnetized Liner Inertial Fusion (MagLIF)* concept

1. A 10–50 T axial magnetic field (B_z) is applied to inhibit thermal conduction losses and to enhance alpha particle deposition

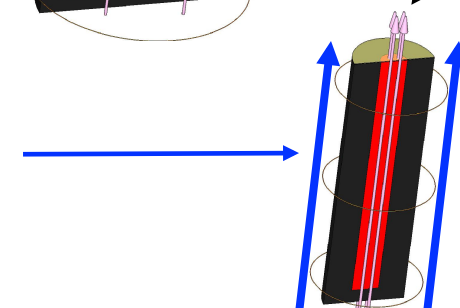


2. ZBL preheats the fuel to ~ 100 – 250 eV to reduce the required compression to $CR \approx 20$ – 30



Z power flow
(A-K gap)

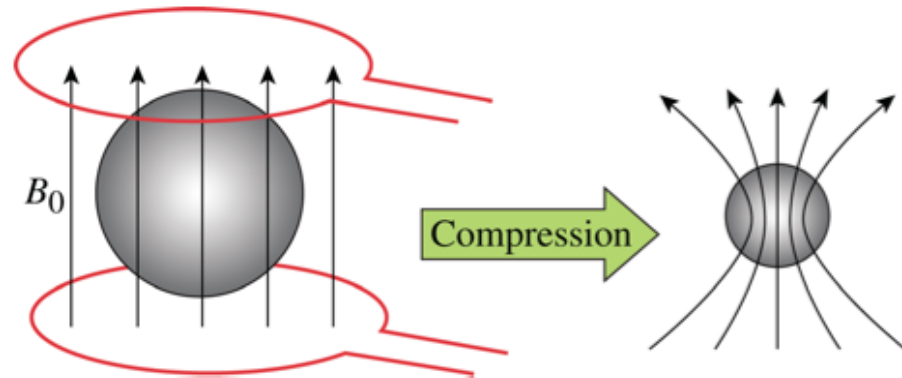
3. Z drive current and B_θ field implode the liner (via z-pinch) at 50–100 km/s, compressing the fuel and B_z field by factors of 1000 in ~ 100 ns



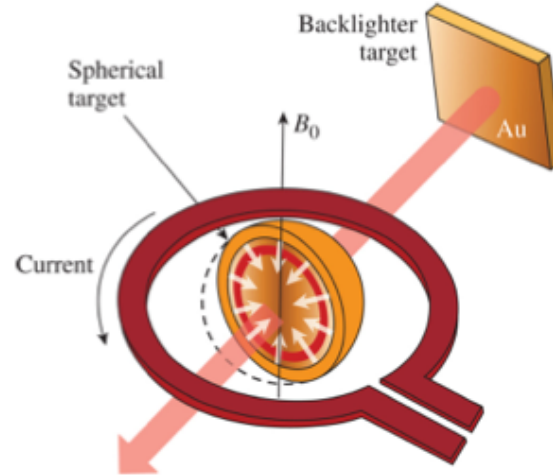
With DT fuel, simulations indicate scientific breakeven may be possible on Z (fusion energy out = energy deposited in fusion fuel)

Recent experiments on OMEGA already have shown benefit of applied B-fields on temps/yields*

Spherical target geometry not optimum for realizing maximum performance gain with a solenoidal B-field, due to field line intersections with cold pusher.



Nevertheless, modest gains in measured ion temperature (15%) and yield (30%) are reported for magnetized (80 kG seed field) direct-drive DD shots. Compressed B-fields near 40 MG.



MagLIF's cylindrical geometry, higher predicted stagnation B-fields and lower hot spot densities suggest greater performance enhancement with fuel magnetization, *including possible suppression of the Knudsen loss mechanism.*

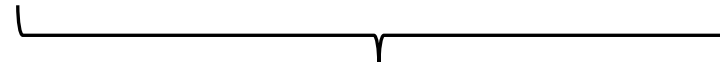
Outline

- Magnetized and cylindrical ICF systems
- Overview of Knudsen loss mechanism
- Heuristic model illustrating impact of applied magnetic field
- Full kinetic equations and model assumptions
- New SDE tail-ion transport particle code
- Qualitative effects of B-field on tail-ion transport
- Exploring the dimensionless parameter landscape
- Ion distribution function anisotropy/inhomogeneity
- Conclusions and future work

Modified tail ion local loss model illustrates the breakdown of enhanced losses at high energies

Review Molvig *et al* local loss model*:

Planar tail ion kinetic equation: $\frac{\partial f_i}{\partial t} + v\mu \frac{\partial f_i}{\partial z} = \frac{1}{2} \nu_{ii}^\mu \frac{v_{Ti}^3}{v^3} \frac{\partial}{\partial \mu} (1 - \mu^2) \frac{\partial f_i}{\partial \mu} + \mathcal{C}_{ii}^E (f_i, f_i)$



Advection + pitch-angle scattering act diffusively (spatially) on short timescales $\approx \mathcal{D} \frac{\partial^2 f_i}{\partial z^2} \approx \frac{\mathcal{D}}{L^2} f_i$ (local loss approximation)

$\mathcal{D} \approx \frac{\Delta z^2}{\Delta t} \approx \lambda_i^2 \nu_{ii}^\mu \approx \frac{v_{Ti}^2}{3 \nu_{ii}^\mu} \varepsilon_k^{5/2}$ (strong energy scaling)

$^* \varepsilon_k = m_i v^2 / 2T_i$

Steady-state local loss model:

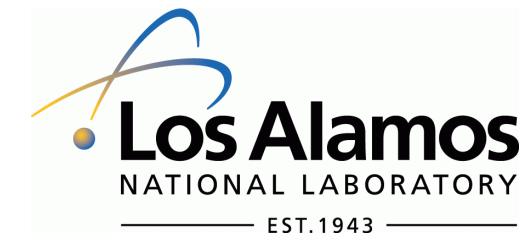
 $0 = \frac{\partial}{\partial \varepsilon_k} \left[f_i + \frac{\partial}{\partial \varepsilon_k} f_i \right] - N_K^2 \varepsilon_k^3 f_i$

$N_K^2 = \frac{1}{3} \frac{v_{Ti}^2}{L^2} \frac{1}{\nu_{ii}^\mu \nu_{ii}^E} \approx \frac{\lambda_i^2}{L^2}$ (Thermal Knudsen number)

Leads to asymptotic solution:

$$f_K \approx \frac{2}{\sqrt{\pi + N_K \varepsilon_k^{3/2}}} \exp \left(-\varepsilon_k - \frac{2}{5} N_K \varepsilon_k^{5/2} \right)$$

Enhanced tail ion depletion!
Maxwellian at low energies, consistent w/ assumptions



Outline

- Magnetized and cylindrical ICF systems
- Overview of Knudsen loss mechanism
- Heuristic model illustrating impact of applied magnetic field
- Full kinetic equations and model assumptions
- New SDE tail-ion transport particle code
- Qualitative effects of B-field on tail-ion transport
- Exploring the dimensionless parameter landscape
- Ion distribution function anisotropy/inhomogeneity
- Conclusions and future work

Modified tail ion local loss model illustrates the breakdown of enhanced losses at high energies

Modified local loss model for transport perpendicular to \mathbf{B} :

Magnetized ions exhibit different spatial step size during diffusive random walk, leading to a modified diffusion coefficient with a different energy scaling

$$\mathcal{D} \approx \rho_L^2 \nu_{ii}^\mu \approx \frac{v_{Ti}^2 \nu_{ii}^\mu}{\omega_{ci}^2} \frac{1}{\varepsilon_k^{1/2}}$$

Modified steady-state local loss model:

$$0 = \frac{\partial}{\partial \varepsilon_k} \left[f_i + \frac{\partial}{\partial \varepsilon_k} f_i \right] - N_B^2 f_i$$

$$N_B^2 = \frac{v_{Ti}^2}{\omega_{ci}^2} \frac{\nu_{ii}^\mu}{\nu_{ii}^E} \frac{1}{L^2} \approx \frac{\rho_L^2}{L^2} \quad (\text{Magnetic Knudsen number})$$

New model has **no asymptotic solution** at high energies.

In fact, exact solution is Maxwellian w/ modified temperature, violating the original assumptions of our model (that only high energy ions deviate from the background Maxwellian by enhanced losses, while low energy ions are unaffected).

Suggests that preferential loss of high energy ions suppressed by magnetic field, mitigating Knudsen mechanism *perpendicular to \mathbf{B}* .

Modified tail ion local loss model illustrates the breakdown of enhanced losses at high energies

Estimated (approximate) threshold conditions for mitigation of Knudsen-depleted reactivities via fuel magnetization (non-resonant reactions; e.g., DD):

1) Magnetization of ions near the Gamow peak energy: $\frac{N_B}{N_K} \lesssim \xi^{3/2}$

2) Adequately large system spatial scale: $N_B \ll \frac{1}{\xi^{1/2}}$

$$^*\xi = 6.2696 (Z_1 Z_2)^{2/3} \left(\frac{A_1 A_2}{A_1 + A_2} \right)^{1/3} [T \text{ (keV)}]^{-1/3} \quad \text{(Gamow factor)}$$

Satisfaction of condition (2) implies that condition (1) can be satisfied easily for values of N_K that normally would produce enhanced depletion ($N_K \sim \mathcal{O}(1)$).

Remarkable result that we expect Knudsen reactivity depletion mechanism to shut off with magnetic fields still too weak to magnetize bulk (thermal) ions.

This is what distinguishes our considerations from those in magnetic fusion: we can have a *highly collisional, essentially unmagnetized* plasma and still obtain a marked performance gains from the presence of relatively modest magnetic fields, through the suppression of e^- heat conduction and Knudsen

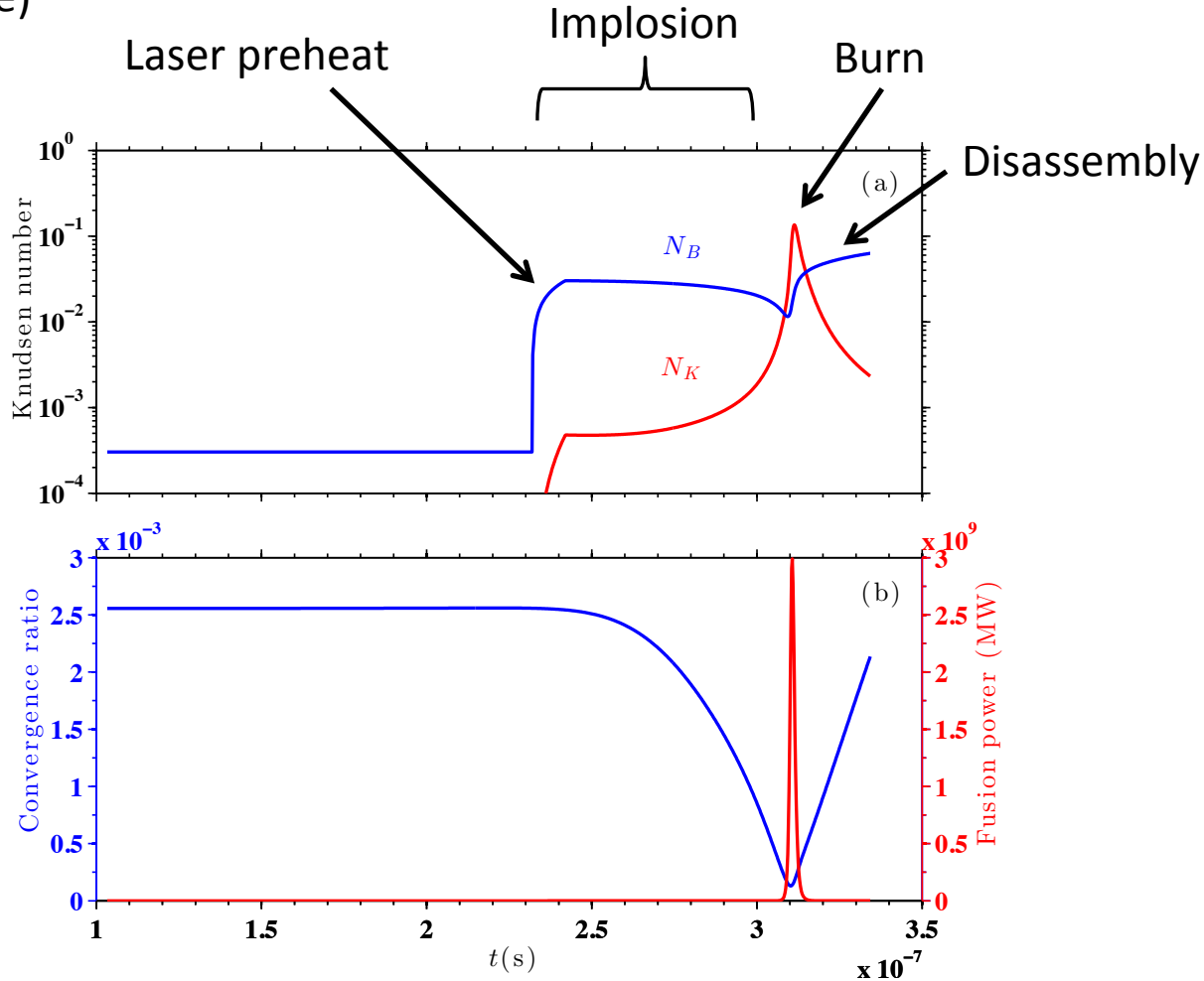
Modified tail ion local loss model illustrates the breakdown of enhanced losses at high energies

Anticipated MagLIF regime found using 0D fully-integrated multiphysics implosion code (Ryan McBride)

* Note that both Knudsen mitigation criteria are satisfied during peak burn in MagLIF implosion

$$1) \frac{N_B}{N_K} \lesssim \xi^{3/2}$$

$$2) N_B \ll \frac{1}{\xi^{1/2}}$$



Outline

- Magnetized and cylindrical ICF systems
- Overview of Knudsen loss mechanism
- Heuristic model illustrating impact of applied magnetic field
- **Full kinetic equations and model assumptions**
- New SDE tail-ion transport particle code
- Qualitative effects of B-field on tail-ion transport
- Exploring the dimensionless parameter landscape
- Ion distribution function anisotropy/inhomogeneity
- Conclusions and future work

Tail-ion kinetic equations and model assumptions

Ion Boltzmann equation: $\frac{\partial f_a}{\partial t} + \mathbf{v} \cdot \nabla f_a + \frac{eZ_a}{m_a} \mathbf{E} \cdot \frac{\partial f_a}{\partial \mathbf{v}} = \mathcal{C}_a(f_a) - \omega_{ca} (\mathbf{v} \times \hat{\mathbf{b}}) \cdot \frac{\partial f_a}{\partial \mathbf{v}}$

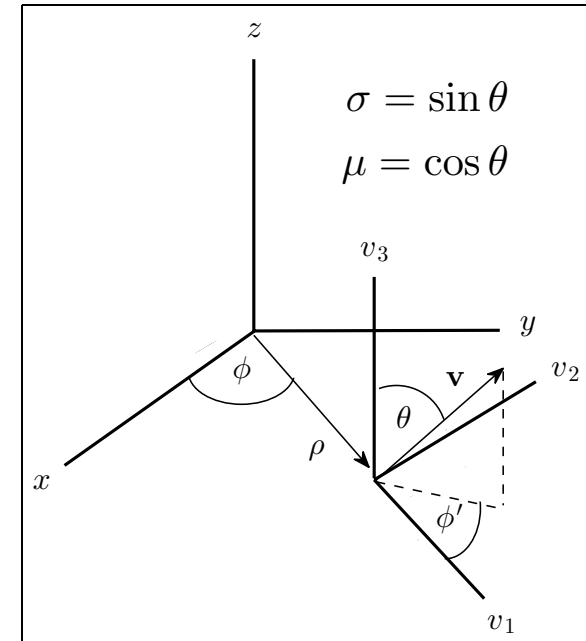
Model assumptions:

- Tail ions non-interacting with one another, so can use linearized test-particle collision operator and prescribe steady-state bulk density, temperature, etc.
- Uniform applied magnetic field: $\mathbf{B} = B\hat{\mathbf{z}}$
- Cylindrically radial ambipolar electric fields: $\mathbf{E} = E(\rho)\hat{\rho}$
- Adopt a hybrid cylindrical/spherical (spatial/velocity) 6D coordinate system (right)

In hybrid coordinates, Fokker-Planck form:

$$\begin{aligned} \frac{\partial f_a}{\partial t} + \frac{1}{\rho} \frac{\partial}{\partial \rho} (\sigma v \rho \cos \phi' f_a) - \frac{\partial}{\partial \phi'} \left(\sigma v \frac{\sin \phi'}{\rho} f_a \right) \\ + \frac{1}{v^2} \frac{\partial}{\partial v} \left(\frac{eZ_a E}{m_a} \sigma v^2 \cos \phi' f_a \right) - \frac{1}{v} \frac{\partial}{\partial \mu} \left(\frac{eZ_a E}{m_a} \sigma \mu \cos \phi' f_a \right) - \frac{\partial}{\partial \phi'} \left[\left(\frac{eZ_a E}{m_a} \frac{\sin \phi'}{\sigma v} + \omega_{ca} \right) f_a \right] \\ = \nu_a^E v_{Ta}^3 \frac{1}{v^2} \frac{\partial}{\partial v} \left[D(v) \left(f_a + \frac{T_a}{m_a} \frac{1}{v} \frac{\partial f_a}{\partial v} \right) \right] + \nu_a^\mu \frac{v_{Ta}^3}{v^3} F(v) \left[\frac{1}{2} \left(\frac{\partial}{\partial \mu} (1 - \mu^2) \frac{\partial f_a}{\partial \mu} + \frac{1}{1 - \mu^2} \frac{\partial^2 f_a}{\partial \phi'^2} \right) \right] \end{aligned}$$

Hybrid coordinate system:



Tail-ion kinetic equations and model assumptions

Further manipulations:

- Convert to dimensionless length, time, velocity, and potential units based on 1 keV, 1 g/cc *reference plasma*.

$$\nu_{\mu 0} \equiv \frac{Z_a^2}{\sqrt{A_a}} \frac{4\pi \rho_{m0} e^4 \langle Z_b^2 \ln \Lambda_{ab} \rangle_0}{m_p^3 v_{T0}^3 \langle A_b \rangle_0} \quad (1/\text{time})$$

$$v_{T0} \equiv \sqrt{\frac{2T_0}{m_a}} \quad (\text{velocity})$$

$$\lambda_{\mu 0} \equiv \frac{v_{T0}}{\nu_{\mu 0}} \quad (\text{length})$$

$$\Phi_0 \equiv \frac{T_0}{e} \quad (\text{potential})$$

- Transform velocity magnitude to energy variable: $\varepsilon_k = u^2 \equiv \frac{v^2}{v_{T0}^2}$
- Define new dependent variable, $F_a \equiv (1/2) \rho \varepsilon_k^{1/2} f_a$, such that number of particles in each differential volume element is given by: $dN = d\rho d\varepsilon_k d\mu d\phi' F_a$
- Factor derivative terms into canonical Fokker-Planck form with clear drag and diffusion contributions for each variable
- Yielding...

Tail-ion kinetic equations and model assumptions

Tail-ion kinetic equation:

$$\frac{\partial F_a}{\partial t} = -\frac{\partial}{\partial \rho} \mathcal{F}_\rho F_a - \frac{\partial}{\partial \phi'} \mathcal{F}_\phi F_a - \frac{\partial}{\partial \mu} \mathcal{F}_\mu F_a - \frac{\partial}{\partial \varepsilon_k} \mathcal{F}_\varepsilon F_a + \frac{1}{2} \frac{\partial^2}{\partial \phi'^2} \mathcal{D}_{\phi\phi} F_a + \frac{1}{2} \frac{\partial^2}{\partial \mu^2} \mathcal{D}_{\mu\mu} F_a + \frac{1}{2} \frac{\partial^2}{\partial \varepsilon_k^2} \mathcal{D}_{\varepsilon\varepsilon} F_a$$

Drag terms $\left\{ \begin{array}{l} \mathcal{F}_\rho = \sigma \varepsilon_k^{1/2} \cos \phi' \\ \mathcal{F}_\phi = \frac{Z_a}{2} \frac{\partial \Phi}{\partial \rho} \frac{\sin \phi'}{\sigma \varepsilon_k^{1/2}} - \sigma \varepsilon_k^{1/2} \frac{\sin \phi'}{\rho} + \chi_a \end{array} \right. \quad {}^* \chi_a \equiv \frac{\omega_{ca}}{\nu_{\mu 0}} \quad (\text{magnetic field only shows up in gyrophase drag term})$

Diffusion terms $\left\{ \begin{array}{l} \mathcal{F}_\mu = \frac{Z_a}{2} \frac{\partial \Phi}{\partial \rho} \frac{\sigma \mu}{\varepsilon_k^{1/2}} \cos \phi' - \frac{\rho_m \Pi_a}{\varepsilon_k^{3/2}} \mu F(\varepsilon_k) \\ \mathcal{F}_\varepsilon = - \left(\frac{2 \rho_m \Pi_a}{\varepsilon_k^{1/2}} A_a \left\langle \frac{1}{A_b} \right\rangle [D(\varepsilon_k) - T_a D'(\varepsilon_k)] + Z_a \frac{\partial \Phi}{\partial \rho} \sigma \varepsilon_k^{1/2} \cos \phi' \right) \end{array} \right.$

$$\mathcal{D}_{\phi\phi} = \frac{\rho_m \Pi_a}{\varepsilon_k^{3/2}} F(\varepsilon_k) \frac{1}{1 - \mu^2}$$

$$\mathcal{D}_{\mu\mu} = \frac{\rho_m \Pi_a}{\varepsilon_k^{3/2}} F(\varepsilon_k) (1 - \mu^2)$$

$$\mathcal{D}_{\varepsilon\varepsilon} = 4 \rho_m \Pi_a T_a A_a \left\langle \frac{1}{A_b} \right\rangle \frac{D(\varepsilon_k)}{\varepsilon_k^{1/2}}$$

$$\begin{aligned} \frac{d\rho}{dt} &= \mathcal{F}_\rho \\ \frac{d\phi'}{dt} &= \mathcal{F}_\phi + \mathcal{D}_{\phi\phi}^{1/2} \Gamma_1(t) \\ \frac{d\mu}{dt} &= \mathcal{F}_\mu + \mathcal{D}_{\mu\mu}^{1/2} \Gamma_2(t) \\ \frac{d\varepsilon_k}{dt} &= \mathcal{F}_\varepsilon + \mathcal{D}_{\varepsilon\varepsilon}^{1/2} \Gamma_3(t) \end{aligned}$$

The formal solution to this equation can be found by solving an equivalent set of single-particle stochastic differential orbital equations for an ensemble of test particles

Tail-ion kinetic equations and model assumptions

Model advantages and limitations:

- Advantages:
 - Test ion formalism + prescribed background plasma = FAST/parallelizable, allowing detailed localized calculations of distribution functions and reactivities
 - Can be generalized easily to include complex background profiles, including inhomogeneous temperatures, densities, fields, and ion species concentrations.
 - Could eventually be used in-line with rad-hydro codes, which would feed in a profile, or be used to construct look-up tables for modified reactivities, etc.
- Limitations
 - No self-consistent evolution of background plasma profile
 - Low energy test ions converge to prescribed background profile (requirement for model validity) only when background profile is a true bulk equilibrium and all macroscopic fields (n, T, E, B) are represented accurately.
 - Not yet clear if time-dependent burn processes can be modeled with similar formalism. SDEs fully time-dependent, but background is formally decoupled.
- Ultimately, model and code will prove to be most powerful when used in conjunction with full multiphysics particle codes (Lsp, VPIC)

Outline

- Magnetized and cylindrical ICF systems
- Overview of Knudsen loss mechanism
- Heuristic model illustrating impact of applied magnetic field
- Full kinetic equations and model assumptions
- **New SDE tail-ion transport particle code**
- Qualitative effects of B-field on tail-ion transport
- Exploring the dimensionless parameter landscape
- Ion distribution function anisotropy/inhomogeneity
- Conclusions and future work

New SDE tail-ion transport particle code

Code features:

- Solves tail-ion transport problem in cylindrical and spherical geometries.
- Includes effects due to presence of homogeneous applied magnetic field.
- Calculates steady-state ion distribution functions in full 6D phase space (if desired) for up to two different *active* ion species at the same time.
- Uses test particles to perform an effective Markov-chain Monte Carlo calculation of fusion reactivities for the active species, including (at this point) DT reactions and both branches of DD reactions.
- Adjustable fuel temperature and density, wall temperature, fuel composition (arbitrary number of ion species), magnetic field strength, target size, diagnostic intervals.
- Outputs include sample particle trajectory data, time-averaged phase space distributions, and spatially resolved fusion reactivities.
- Written in C, parallelized with MPI. Have run on 1600 processors, highly scalable.

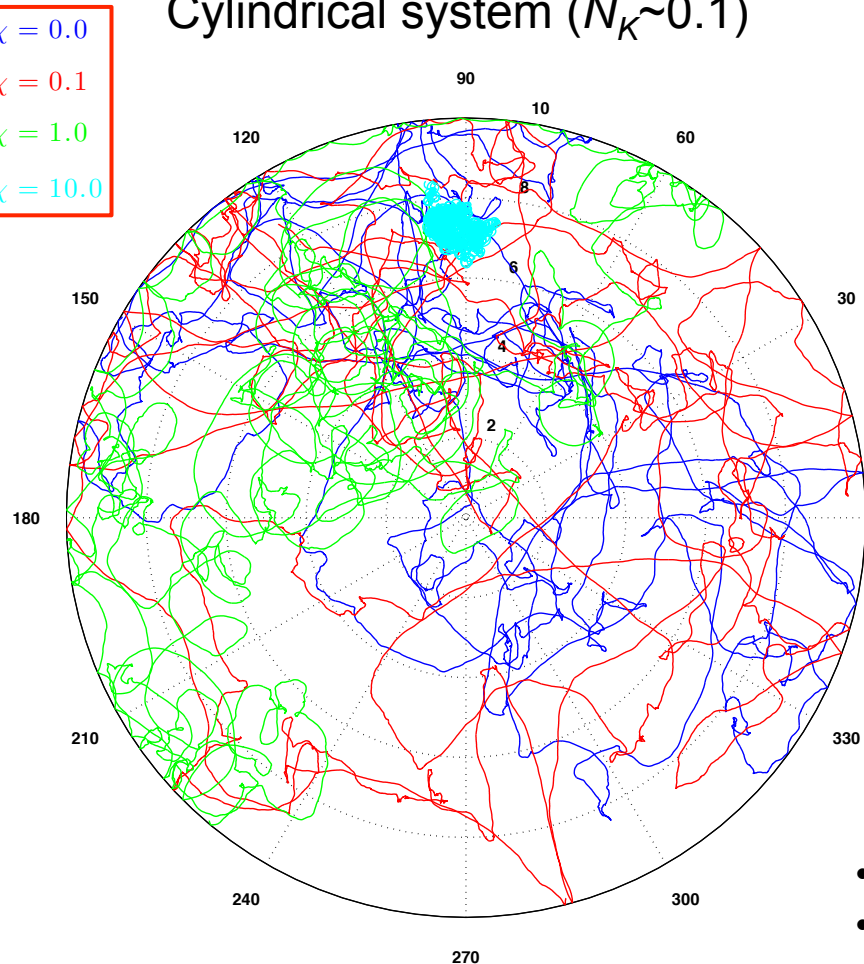
Outline

- Magnetized and cylindrical ICF systems
- Overview of Knudsen loss mechanism
- Heuristic model illustrating impact of applied magnetic field
- Full kinetic equations and model assumptions
- New SDE tail-ion transport particle code
- Qualitative effects of B-field on tail-ion transport
- Exploring the dimensionless parameter landscape
- Ion distribution function anisotropy/inhomogeneity
- Conclusions and future work

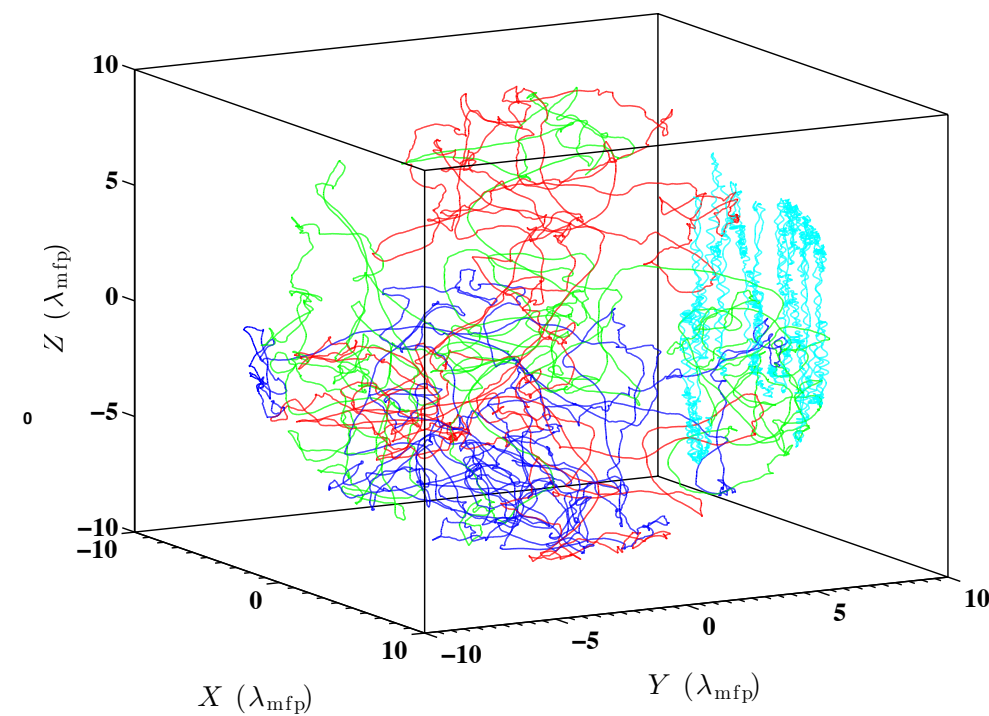
Qualitative effects of B-field on tail-ion transport

Sample ion trajectories with varying magnetizations:

Cylindrical system ($N_K \sim 0.1$)



Spherical system ($N_K \sim 0.1$)



- Ergodicity evident, especially with weaker \mathbf{B}
- Direct signature of marginal magnetization difficult to detect from trajectories, but appears clearly in ensemble statistics (addressed in next section)

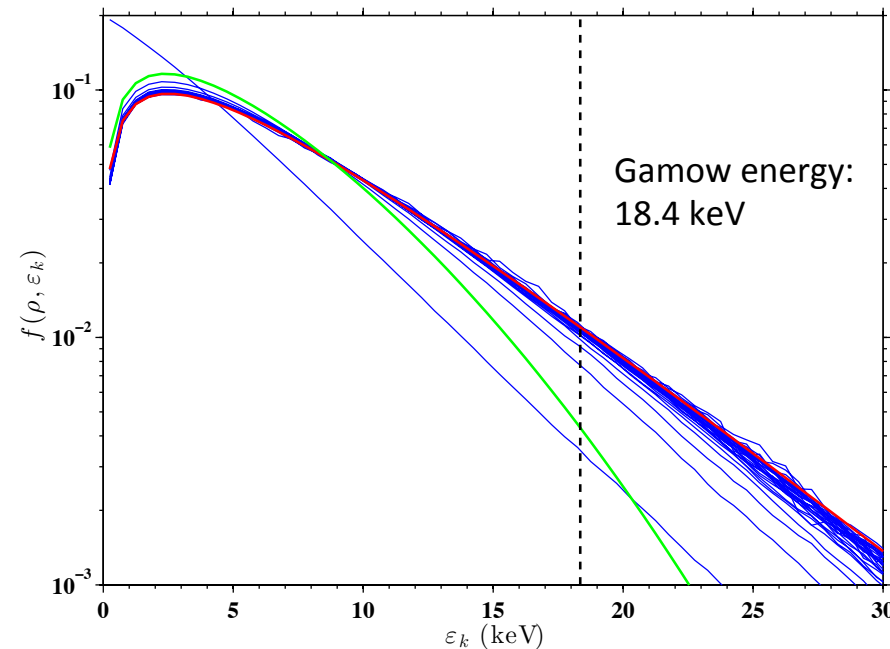
* χ defined alternatively as : $\chi \equiv \frac{\omega_{ca}}{\nu_{\mu a}}$

Qualitative effects of B-field on tail-ion transport

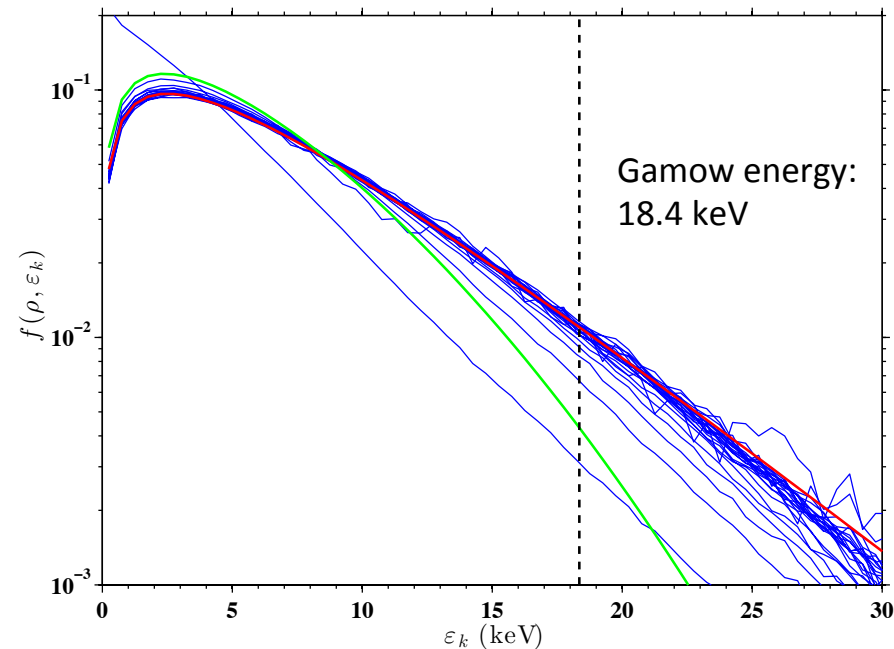
Distribution function vs. radial position: 5 keV, 1 g/cc, DD plasma, $N_K \sim 0.1$, 10 eV wall

$$\chi = 0$$

Cylindrical system



Spherical system



Red line: Maxwellian distribution

Green line: Analytical Knudsen solution (unmagnetized) [Molvig *et al*, PRL 109, 095001 (2012)]

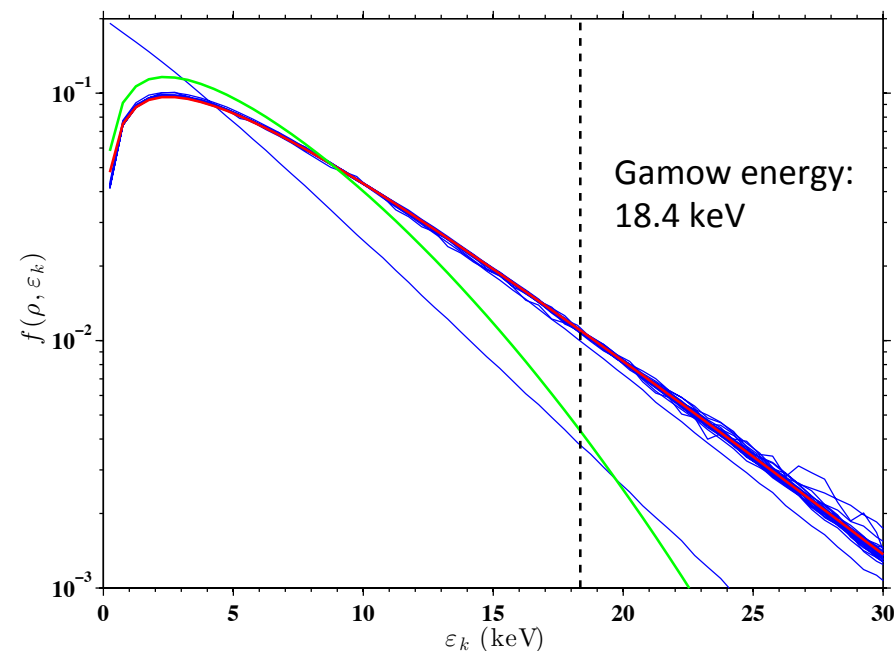
- Knudsen tail-ion depletion more pronounced in spherical geometry compared to cylindrical geometry
- Analytical model seems to overestimate depletion scaling significantly, particularly for core plasma
- Evidence of distribution function anisotropy close to wall in spherical geometry case
- Ion transport model assumptions validated, even very close to cold wall, esp. for cylindrical systems

Qualitative effects of B-field on tail-ion transport

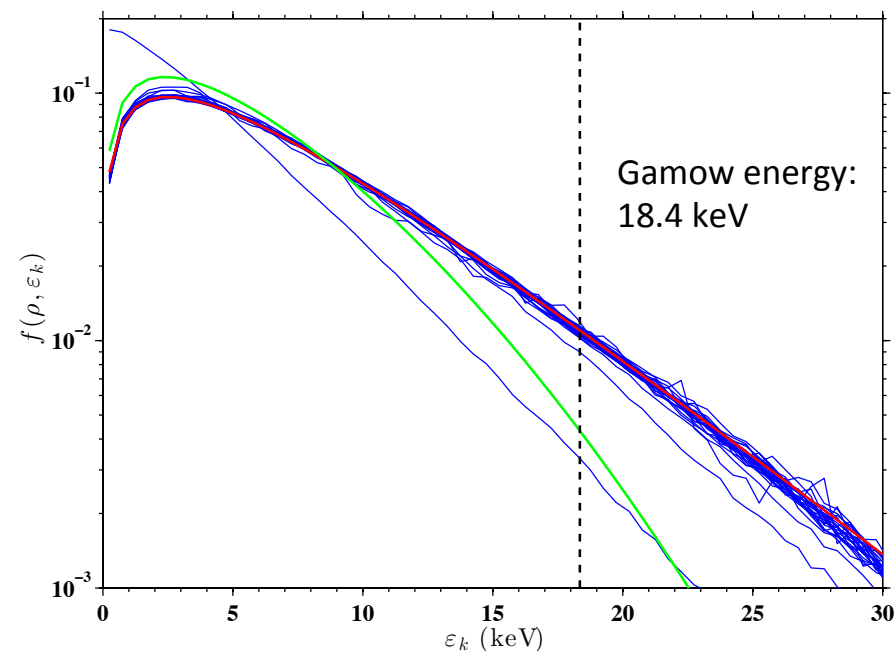
Distribution function vs. radial position: 5 keV, 1 g/cc, DD plasma, $N_K \sim 0.1$, 10 eV wall

$$\chi = 5$$

Cylindrical system



Spherical system



Red line: Maxwellian distribution

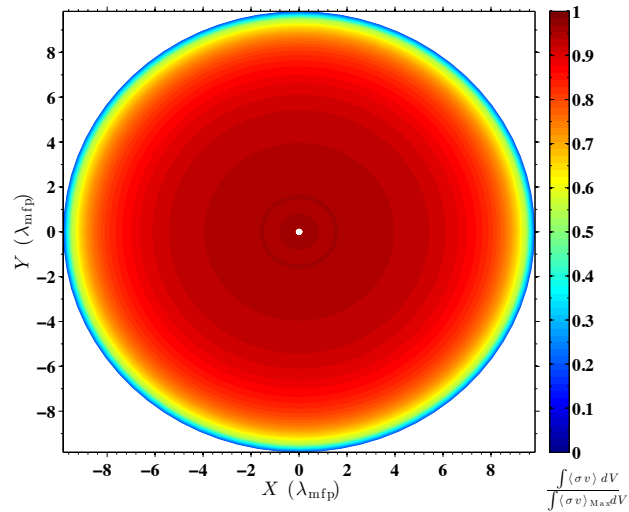
Green line: Analytical Knudsen solution (unmagnetized) [Molvig *et al*, PRL 109, 095001 (2012)]

- Knudsen depletion mitigated substantially with magnetization in cylindrical system
- Tail depletion improved in spherical system with magnetization, but not to the same extent as cylindrical system, due to less ideal target geometry to take advantage of solenoidal B-field.

Qualitative effects of B-field on tail-ion transport

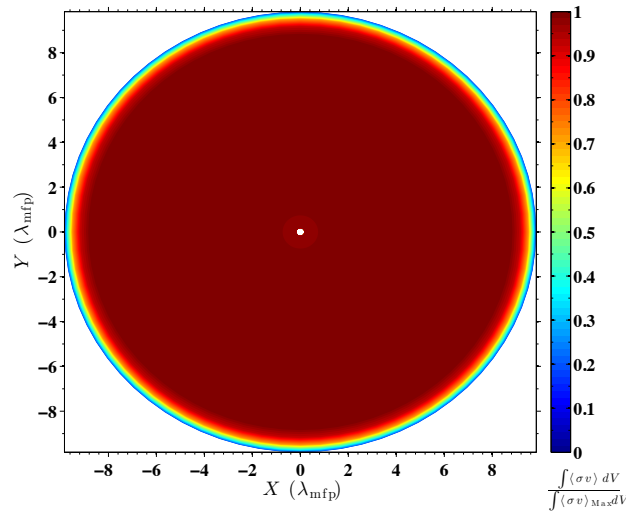
Cylindrical system: 5 keV, 1 g/cc, DD plasma. **Strong B nearly eliminates Knudsen!**

Global reactivity vs. Maxwellian: 0.80



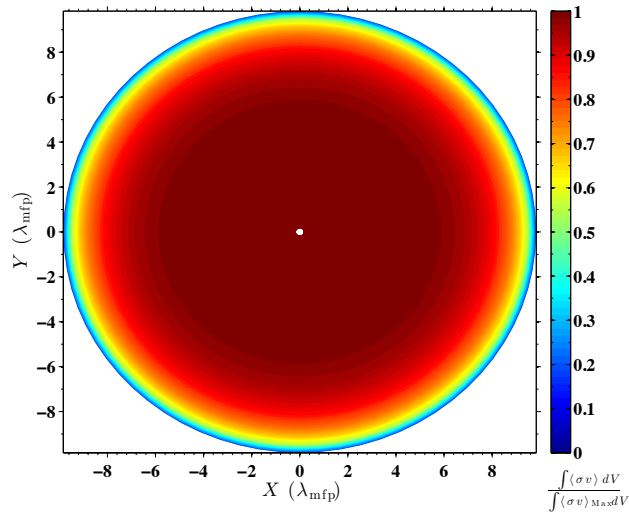
$\chi = 0$

Global reactivity vs. Maxwellian: 0.93



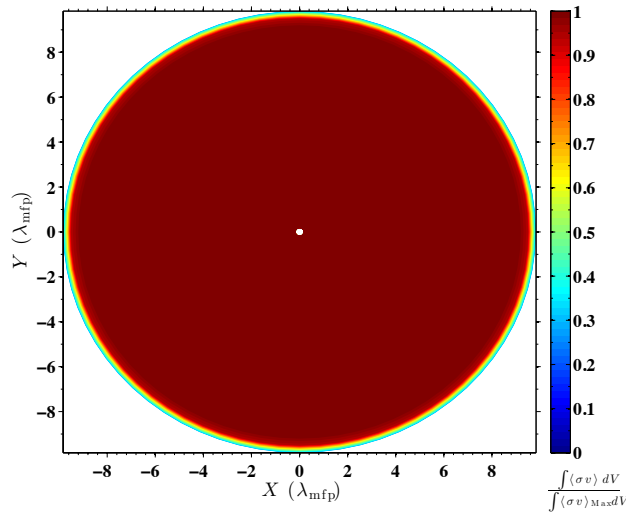
$\chi = 5$

Global reactivity vs. Maxwellian: 0.85



$\chi = 1$

Global reactivity vs. Maxwellian: 0.95

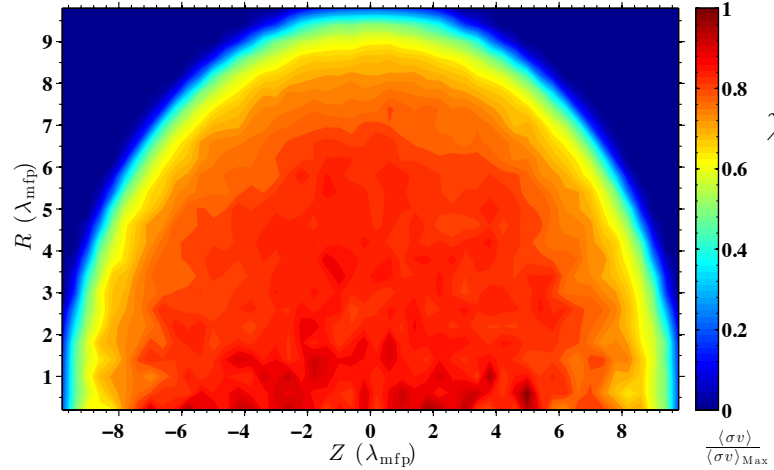


$\chi = 10$

Qualitative effects of B-field on tail-ion transport

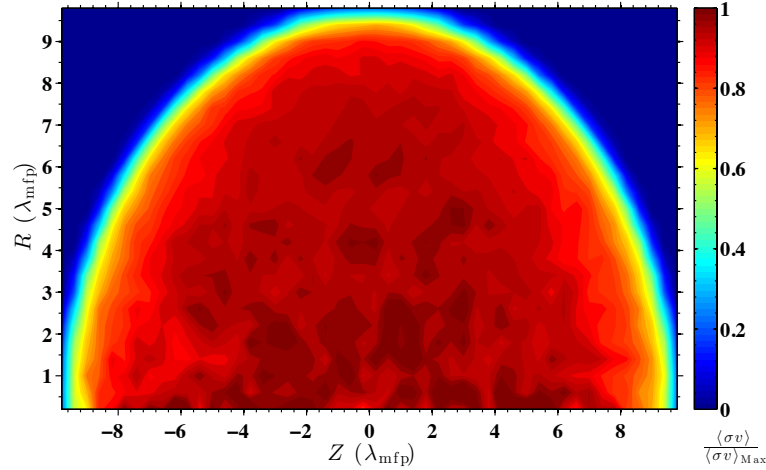
Spherical system: 5 keV, 1 g/cc, DD plasma. **Benefit from stronger B saturates!**

Global reactivity vs. Maxwellian: 0.65



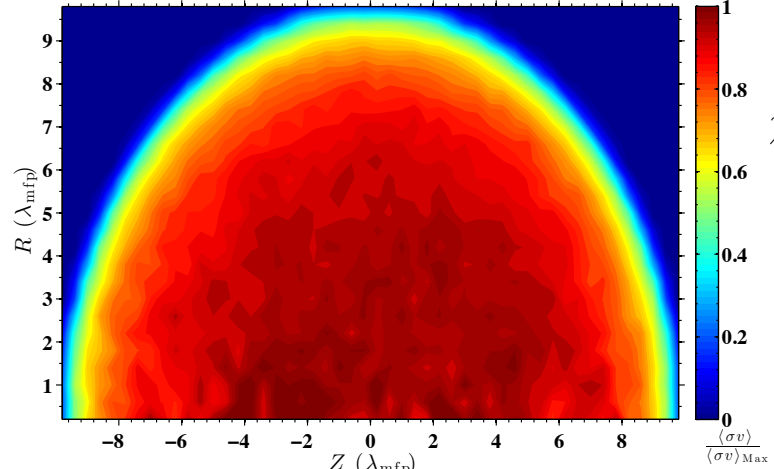
$\chi = 0$

Global reactivity vs. Maxwellian: 0.77



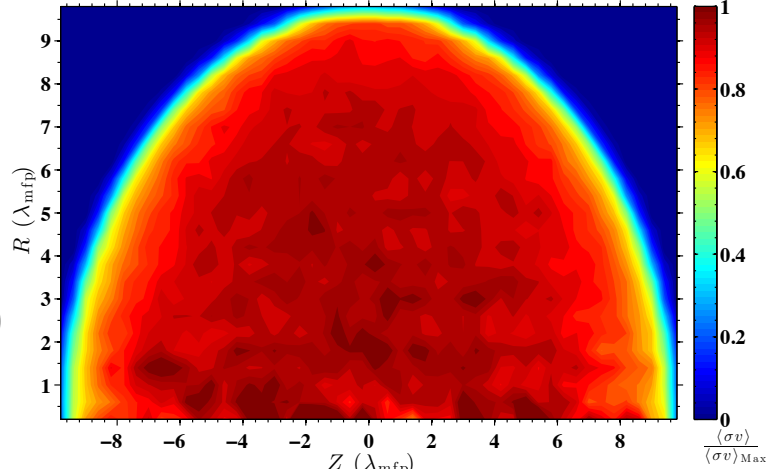
$\chi = 5$

Global reactivity vs. Maxwellian: 0.72



$\chi = 1$

Global reactivity vs. Maxwellian: 0.77



$\chi = 10$

Outline

- Magnetized and cylindrical ICF systems
- Overview of Knudsen loss mechanism
- Heuristic model illustrating impact of applied magnetic field
- Full kinetic equations and model assumptions
- New SDE tail-ion transport particle code
- Qualitative effects of B-field on tail-ion transport
- **Exploring the dimensionless parameter landscape**
- Ion distribution function anisotropy/inhomogeneity
- Conclusions and future work

Exploring the dimensionless parameter landscape

Cylindrical system: 8 keV, 1 g/cc, DD plasma: volume-averaged reactivity reduction

Predicted Knudsen mitigation criteria:

$$\frac{N_B}{N_K} \lesssim \xi^{3/2} \quad N_B \ll \frac{1}{\xi^{1/2}}$$

$$*(\xi \approx 3.1)$$

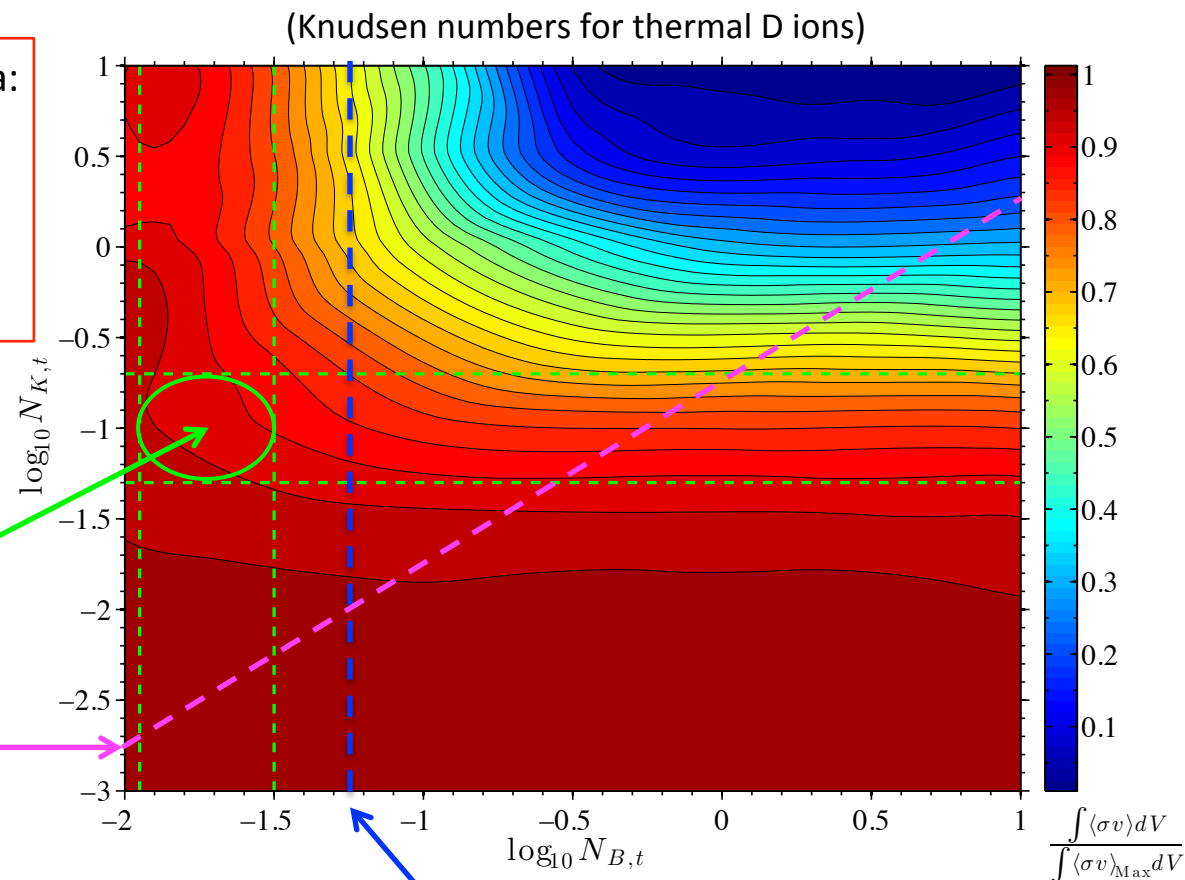
**MagLIF point
design should
exhibit suppressed
Knudsen tail
depletion via tail-
ion magnetization**

$$\left. \begin{aligned} N_K &\sim \frac{\lambda_{\text{mfp}}}{L} \sim \frac{T^2}{nL} \\ N_B &\sim \frac{\rho_L}{L} \sim \frac{T^{1/2}}{BL} \end{aligned} \right\}$$

MagLIF operating regime

$$\frac{N_B}{N_K} = \xi^{3/2}$$

Scan (N_K, N_B) -space at
fixed T, n by varying B, L .



$$N_B = 0.1 \left(\frac{1}{\xi^{1/2}} \right)$$

Exploring the dimensionless parameter landscape

Spherical system: 8 keV, 1 g/cc, DD plasma: volume-averaged reactivity reduction

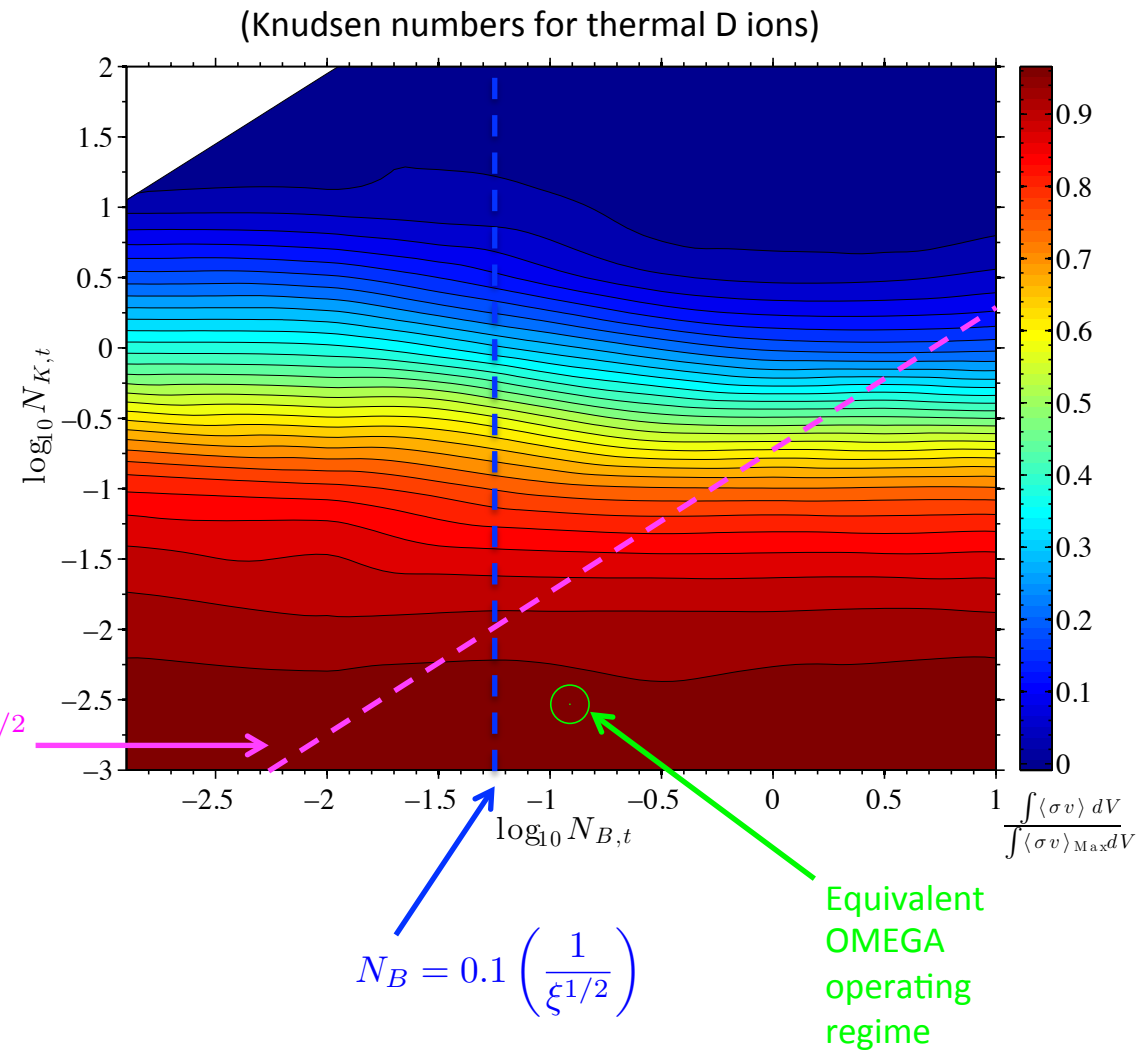
Predicted Knudsen mitigation criteria:

$$\frac{N_B}{N_K} \lesssim \xi^{3/2} \quad N_B \ll \frac{1}{\xi^{1/2}}$$

$^*(\xi \approx 3.1)$

Magnetized OMEGA experiments not in regime where B-field impacts Knudsen mechanism significantly

Clearly only a limited benefit provided by magnetic field in spherical geometry. Essentially a transition from 3D to 1D depletion

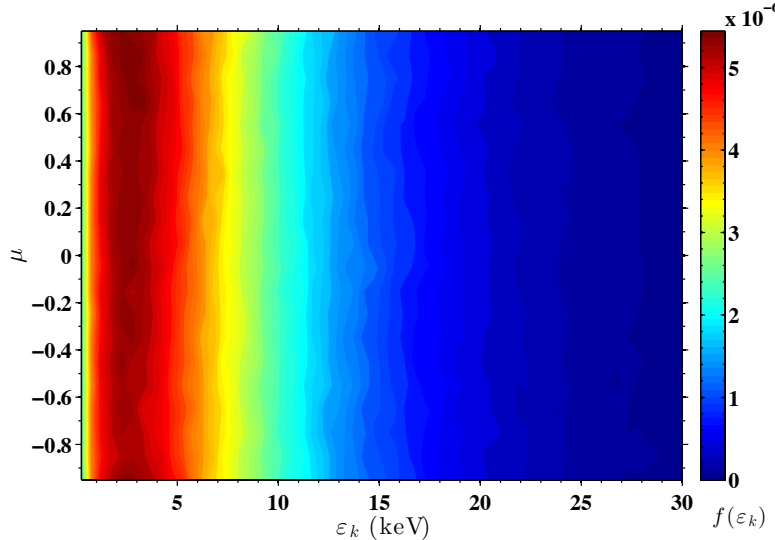


Outline

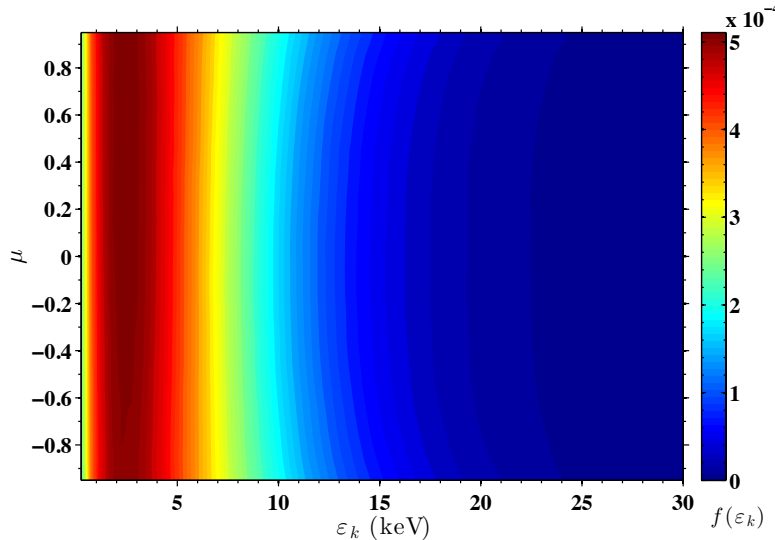
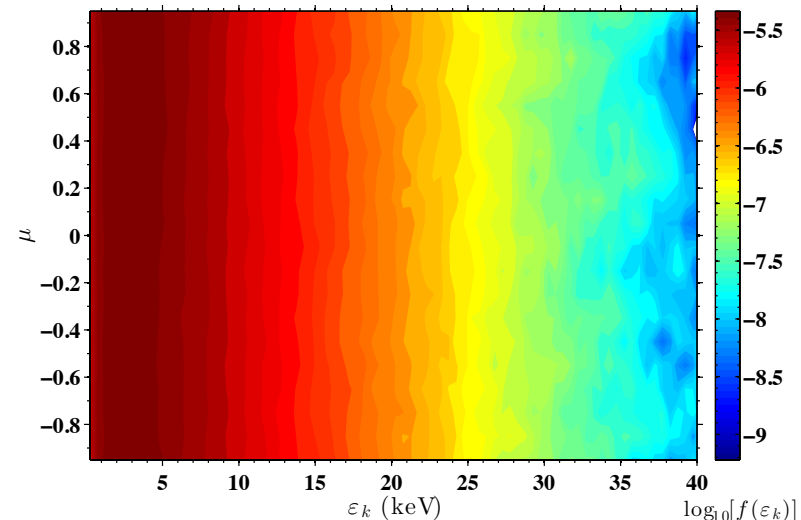
- Magnetized and cylindrical ICF systems
- Overview of Knudsen loss mechanism
- Heuristic model illustrating impact of applied magnetic field
- Full kinetic equations and model assumptions
- New SDE tail-ion transport particle code
- Qualitative effects of B-field on tail-ion transport
- Exploring the dimensionless parameter landscape
- Ion distribution function anisotropy/inhomogeneity
- Conclusions and future work

Ion distribution function anisotropy/ inhomogeneity

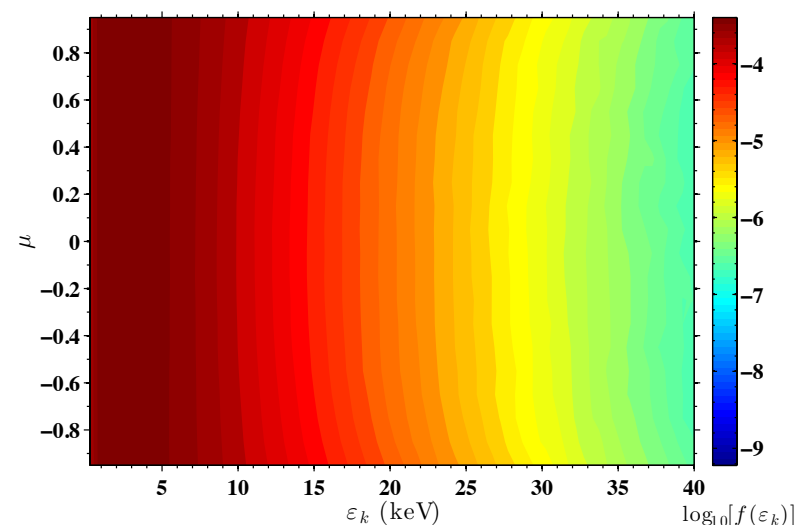
Unmagnetized cylinder: core plasma isotropic, edge plasma depleted near $\mu \approx 0$



Core
plasma

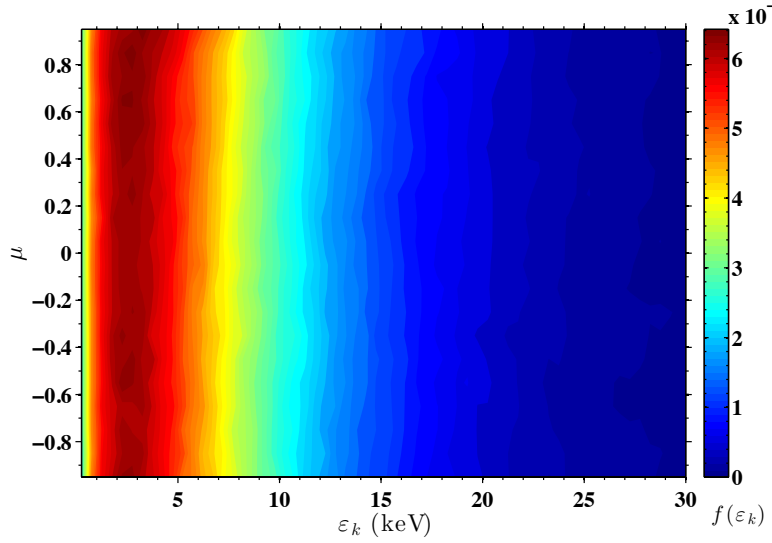


Edge
plasma

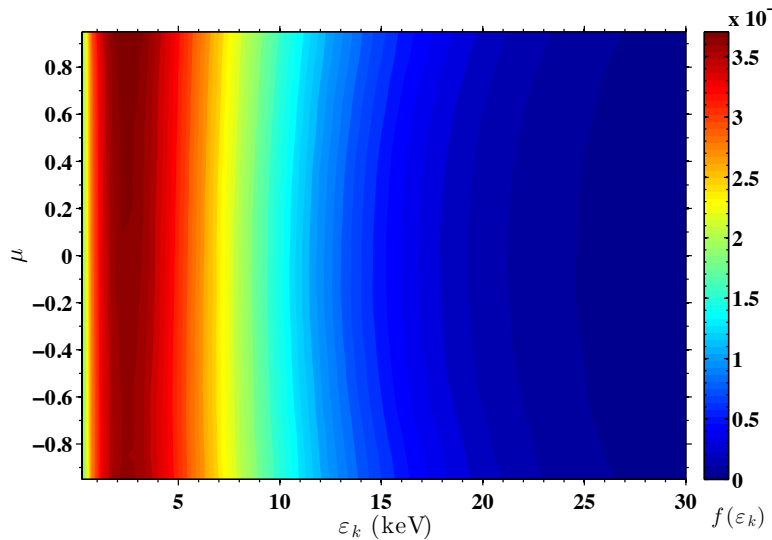
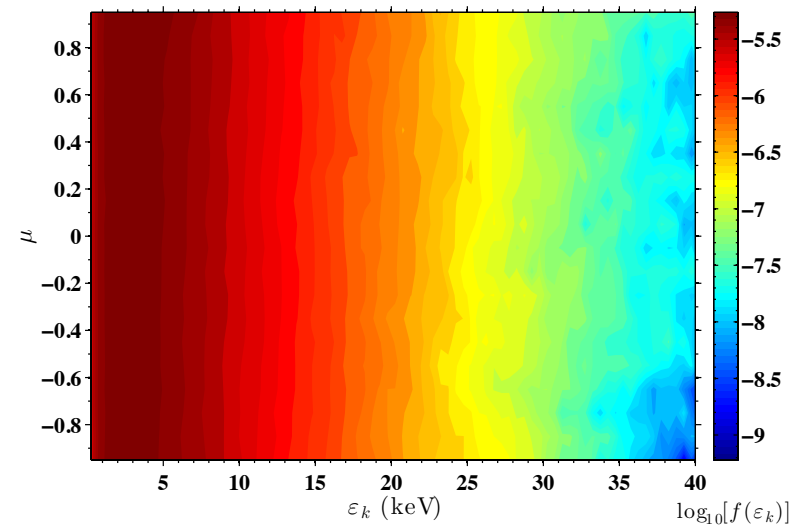


Ion distribution function anisotropy/ inhomogeneity

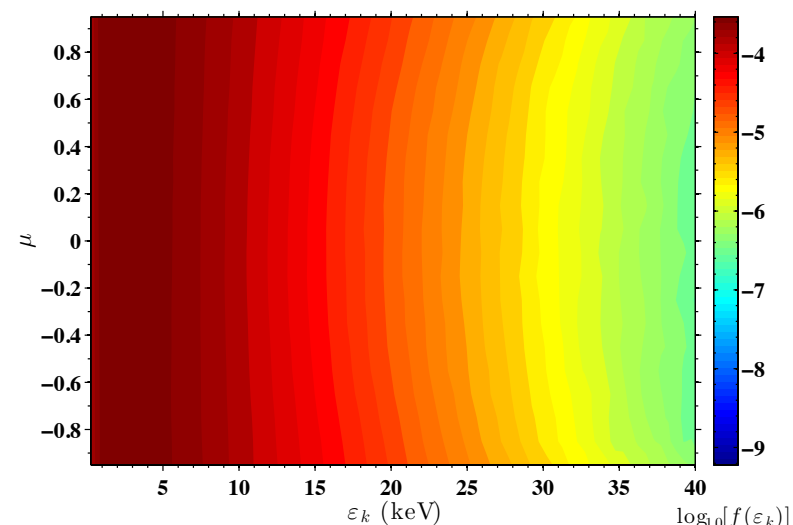
Magnetized cylinder ($\chi = 5$): same edge anisotropy, but confined to narrower region



Core
plasma



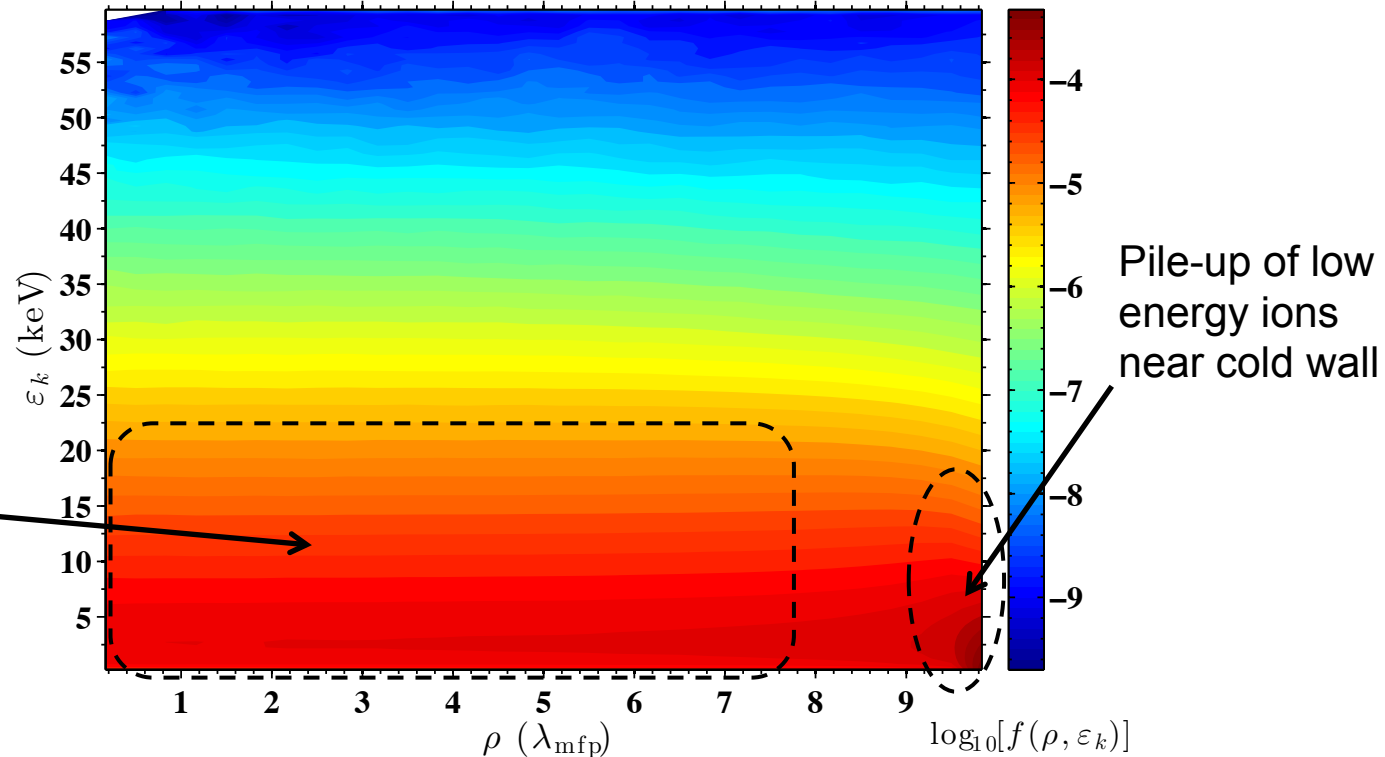
Edge
plasma



Ion distribution function anisotropy/ inhomogeneity

Distribution function for cylindrical DD plasma, 5 keV,
1 g/cc, unmagnetized, with 10 eV wall temperature

Relatively uniform
low energy ion
profile in “core”
plasma



- Low-energy ion distribution deviates substantially from prescribed uniform, hot plasma background *near the cold wall*, violating validity constraint for our model in this region.
- Uniform hot plasma bounded by a cold wall (with infinite temperature gradient across the boundary) **is not a true plasma equilibrium**. Thus, test particles equilibrate to macroscopic forces that don't produce a perfect match to the assumed background conditions at low energy.

Outline

- Magnetized and cylindrical ICF systems
- Overview of Knudsen loss mechanism
- Heuristic model illustrating impact of applied magnetic field
- Full kinetic equations and model assumptions
- New SDE tail-ion transport particle code
- Qualitative effects of B-field on tail-ion transport
- Exploring the dimensionless parameter landscape
- Ion distribution function anisotropy/inhomogeneity
- **Conclusions and future work**

Conclusions

- Heuristic model for tail-ion collisional diffusion perpendicular to a magnetic field suggests magnetic field eliminates *enhanced* losses of high energy ions.
- Full test-ion kinetic equations developed in hybrid cylindrical-spherical coordinates, including applied B-fields, ambipolar E-fields, and arbitrary background plasma temperatures, densities, and ion species concentrations.
- Numerical code developed in C/MPI to solve SDE form of kinetic tail-ion equations in both cylindrical and spherical spatial geometries.
- Analytical Knudsen depletion model (Molvig *et al*, PRL 2012) seems to overestimate the energy scaling of tail depletion, especially in core plasma.
- Uniform magnetization is observed to restore full Maxwellian reactivities throughout fuel region in cylindrical geometries.
- Uniform magnetization provides positive but limited benefit in spherical geometries.
- Estimated threshold conditions for onset of Knudsen mechanism mitigation with magnetization seem to be correct.
- Early magnetized OMEGA experiments do not appear to be a good test case to explore mitigation of Knudsen depletion mechanism.
- Ion distribution isotropic in core plasma, while edge plasma exhibits only very minor anisotropy and enhanced depletion for wall-directed velocities.

Future work

- Further code development:
 - Work on incorporating inhomogeneous temperatures, densities, and fields into background plasma profiles.
 - Investigate possibility of coupling with recently developed Monte Carlo code to model neutron spectra from non-Maxwellian ion distributions [P. F. Knapp *et al*, *Diagnosing Suprathermal Ion Populations in Z-Pinch Plasmas Using Fusion Neutron Spectra*, to appear in Phys. Plasmas].
 - Investigate possibility of modeling time-dependent processes in sub-ignition-scale ICF plasmas, such as burn product transport and secondary nuclear reactions.
- Investigate potential to generate look-up tables for integration with rad-hydro codes
- Develop methods to extract background plasma profiles from existing rad-hydro and particle-in-cell codes and use as input for SDE code.
- Explore steady-state numerical solution adherence to validity constraints in increasingly inhomogeneous environments.
- In general, apply code to search for regimes exhibiting enhanced reactivity and target performance in all relevant ICF settings.